LEGIBILITY NOTICE

A major purpose of the Technical Information Center is to provide the broadest dissemination possible of information contained in DOE's Research and Development Reports to business, industry, the academic community, and federal, state and local governments.

Although a small portion of this report is not reproducible, it is being made available to expedite the availability of information on the research discussed herein.

CONF-8905226--1

LA-UR -89-3265

OCT 1989

LA-UR--89-3265

DE90 000680

TITLE: EFFECTS OF SPATIAL ATTENTION ON THE VISUAL-EVOKED NEUROMAGNETIC RESPONSE

AUTHOR(S): Aine, C.J., LS-1
George, J.S., LS-1
Oakley, M.T., P-6
Medvick, P.A., MEE-3
Flynn, E.R., P-6

SUBMITTED TO: Ninth International Conference on Event-related Potentials of the Brain
May 28 - June 3, 1989
Noordwijk, The Netherlands

EFFECTS OF SPATIAL ATTENTION ON THE VISUAL-EVOKED NEUROMAGNETIC RESPONSE.

AINE, C.J., GEORGE, J.S., OAKLEY, M.T., MEDVICK, P.A., AND FLYNN, E.R.

Life Sciences and Physics Divisions. Los Alamos National Laboratory. MS M-715.
Los Alamos, NM 87545.

Running title: ERFs and visual spatial attention

Send proofs to:

Cheryl Aine, Ph.D.
Life Sciences and Physics Divisions
Mail Stop M-715
Los Alamos National Laboratory
Los Alamos, NM 87545

(505) 665-2545

Key Words: Event-related magnetic fields, Visual spatial attention, Source Localization

Heading: MEG / ATTENTION

Introduction

A number of studies have shown that selective attention to spatial location modulates the amplitudes of several visual evoked potential components recorded from posterior regions of the head (e.g., Eason, Harter & White, 1969; Harter, Aine, & Schroeder, 1982; Hillyard & Munte, 1984; Mangun & Hillyard, 1988). The early components, P1 and N1 (peak latencies: 90-135 and 140-170 msec, respectively), are thought to arise in one or more areas of visual cortex. Although it is generally assumed that such ERP effects reflect differential activation of populations of neurons at successive levels of the nervous system, little information is available about the neural structures responsible for such effects. We have employed neuromagnetic techniques in an attempt to identify more precisely the neural structures involved in selective attention to spatial location within the P1-N1 time sequence. In this study, effects of attention were assessed by comparing neural responses evoked by stimuli at a specified spatial location when subjects were required to attend and respond behaviorally to that location with neural responses to the same stimuli when subjects were required to attend and respond behaviorally to another location in the visual field.

Methods

Subjects and Procedure:

The results reported here were from studies examining effects of selectively attending to sinusoidal gratings presented at different locations in the visual field. Vertical sinusoidal gratings (1 or 5 cycles per degree) were randomly presented at either 1) 0^{o} or 7^{o} along the horizontal meridian in the right visual field or 2) 2^{o} or 5^{o} in the lower left and right visual fields. Extensive neuromagnetic maps were obtained from two subjects for each stimulus set (one subject participated in both experiments). Stimulus duration was 100 msec; the interstimulus interval ranged from 800-1200 msec. Subjects were instructed to respond with their index finger (contralateral to field of target stimulation) to a specific stimulus type (e.g., a 1 cpd grating at 2^{o} in the lower right field) during a block of trials (25 presentations of each stimulus type). Each condition was replicated 2 or 3 times.

Neuromagnetic recordings and analyses:

Neuromagnetic responses were recorded with a 7-channel SQUID-coupled gradiometer system in a magnetically shielded chamber. Sensors were located on a 2 cm triangular grid, one in the center and six in the surround. Neuromagnetic measurements were made at 6-16 contiguous array locations constituting a grid of 42-112 separate sensor locations. Electrical responses (ERPs) were recorded simultaneously. Amplitudes were measured from the prestimulus baseline at 10 msec intervals and iso-contour plots of field distributions were prepared at each latency by weighted interpolation across sensor locations. If the magnetic field maps had roughly symmetric positive and negative peaks, the data were fit with a single equivalent current dipole (ECD) model using nonlinear least squares minimization techniques. This model yields the location, orientation and the strength of the current dipole that best accounts for the data. If more than two extrema were apparent in the observed field distribution and/or the residual field distribution showed extrema exceeding the noise level by at least 2 standard deviations, a 2-Dipole ECD model was applied (see Aine et al. 1989, for details). Theoretical field distributions were derived by forward calculations using parameters of the best-fitting ECD model.

Monte Carlo techniques were used to simulate the effects of magnetic noise on the source localization process by adding random noise (calculated from the 100 msec prestimulus baseline) to observed field amplitudes and fitting the resulting distributions to produce an ensemble of ECDs (see Medvick et al. 1989). These techniques also allowed for statistical evaluation and comparison of the ECD parameters (location, orientation, and moment) for attend versus not attend conditions.

Results

Figure 1 shows representative field distributions for one subject when a 1 cpd grating, presented 2° in the lower right quadrant, was task relevant. At 110 msec a dipole-like configuration is evident in the left hemisphere when the right field was stimulated (empirical fields--left column). The zero crossing between the negative and positive peaks represents the approximate location of the ECD. Positive peaks represent magnetic flux leaving the head while negative peaks reflect re-entering fields. The arrows in the right column represent the

- -

Insert Figure 1 about here

- -

approximate location of the ECDs for the forward field calculation. Goodness-of-fit measures based on chi-square statistics and visual comparison between empirical and theoretical field distributions suggest the ECD is a reasonable model for this case. At 110 msec the single ECD model accounted for 68% of the variance in the actual data while at 160 msec, the 2-dipole ECD model shown in the second row accounted for 62% of the variance. The bar graphs at the bottom of Figure 1 depict the strengths of the ECDs for the attend and not attend conditions for this subject when stimuli were presented at 2° in both left and right fields. The differences exceed 2 standard deviations. The contralateral source strengths at 160 msec were not statistically different (not shown).

Figure 2 illustrates scatterplots of Monte Carlo source calculations for 160 msec, plotted in orthographic projections of the head volume. Note that these projections are not equivalent to surface (Mercator) projections used in contour plots. No clear separation exists between calculated sources for attend and not attend conditions in any view for either ipsilateral or contralateral sources. The clustering of the dipole solutions demonstrate the stability of the solutions.

- -

Insert Figure 2 about here

- -

Figure 3 shows field distributions at 150 msec for attend or not attend presentations of a 1 cpd grating at 7^{o} along the horizontal meridian in the right visual field. Both left and right hemisphere sources were evident in the field distribution when the stimulus was task relevant (Top row). However, when the stimulus was not task relevant an ipsilateral (right hemisphere) source could not be identified. A 2-Dipole model accounted for 78% of the variance when the stimulus was task relevant; a single dipole model accounted for 66% of the variance.

- -

Insert Figure 3 about here

- -

Discussion

Initial contralateral activation was evident for all subjects and for all eccentric placements of the stimulus. This activation was first apparent in distributions at 90-100 msec and dipole-like activity was observed continuously until approximately 160 msec. When the stimulus was task relevant an ipsilateral source was evident at 120 msec and peaked around 140-160 msec. When the stimulus was not task relevant, the ipsilateral source could not be identified in some cases; in other cases a source of reduced strength was evident. These data suggest that the electrical N140-N160 may reflect the summation of at least two (left and right hemisphere) sources. Effects of attention on the initial contralateral sources were apparent around 100-130 msec. Ipsilateral source strengths showed significant effects of attention at 140-160 msec, whereas the contralateral sources no longer showed significant effects of attention at this latency.

Magnetic Resonance Images (MRIs) were obtained for two of the three subjects. Taking into account sensor localization errors in current procedures (+/- .5 cm), the initial contralateral ECD sources are consistent with generators in VI or V2, whereas the ipsilateral sources are clearly extrastriate in origin. This pattern of initial contralateral activity and delayed ipsilateral activation with reduced amplitude, was observed for both left and right field stimulation. These observations are consistent with results reported by Rugg, Lines & Milner (1984) and may reflect the inter-hemispheric transfer of information via the corpus callosum. By examining ratios of ECD moments for attend/not attend conditions for the ipsilateral and contralateral sources we may be able to determine whether attention modulates the inter-hemispheric transfer of activity or simply modulates activity at the level of initial cortical projection.

Acknowledgements

The authors wish to thank Chris Wood for comments on the manuscript, the Center for Non-Invasive Diagnosis, University of New Mexico Medical Center and the Veteran's Administration for MRIs. This work was supported by the U.S. Army Research Institute, Alexandria VA, the U.S. Department of Energy contract W-7405-ENG-36, and by the VA/LANL/UNM Clinical Magnetoencephalography Program.

References

Aine, C., George, J., Medvick, P., Supek, S., Flynn, E. & Bodis-Wollner, I. (in press) Identification of multiple sources in transient visual evoked neuromagnetic responses. In S.J. Williamson (Ed.). Biomagnetism 1989.

Eason, R.G., Harter, M.R. & White, C.T. (1969). Effects of attention and arousal on visually evoked cortical potentials and reaction time in man. Physiology and Behavior, 4, 283-289.

Harter, M.R., Aine, C. & Schroeder, C. (1982). Hemispheric differences in the neural processing of stimulus location and type: Effects of selective attention on visual evoked potentials. Neuropsychologia, 20, 421-438.

Hillyard, S.A. & Munte, T.F. (1984). Selective attention to color and locational cues: An analysis with event-related brain potentials. Perception & Psychophysics, 36, 185-198.

Mangun, G.R. & Hillyard, S.A (1988). Spatial gradients of visual attention: Behavioral and electrophysiological evidence. Electroenceph. clin. Neurophysiol., 70, 417-428.

Medvick, P., Lewis, P.S., Aine, C.J. and Flynn, E.R. (in press). Monte Carlo analysis of localization errors in magnetoencephalography. In S.J. Williamson (Ed.). Biomagnetism 1989.

Rugg, M.D., Lines, C.R. & Milner, D.A. (1984). Visual evoked potentials to lateralized visual stimuli and the measurement of interhemispheric transmission time. Neuropsychologia, 22, 215-225.

Figure Captions

Figure 1. Top: Sample neuromagnetic field distributions for one subject (MO) when a 1 cpd grating, centered 2^o to the right of the vertical meridian and below the horizontal meridian, was task relevant. The origin (x=0, y=0) of these head-surface maps is at the inion. Each averaged response contains 75 individual responses. Bottom: Bar graphs summarize significant effects of selectively attending to gratings presented 2^o in both lower left and right quadrants of the visual field.

Figure 2. Results of Monte Carlo error analyses utilized for examining whether source locations and orientations changed as a function of selective attention. Both contralateral and ipsilateral sources are shown when left and right fields were stimulated. In this head-centered system, the positive z axis is directed through the top of the head, positive y is directed through the left periauricula (i.e., positive y represents left hemisphere activity and negative y reflects right hemisphere activity), and positive x is directed through the nose.

Figure 3. Field distributions at 150 msec are shown for subject LP when the grating was task relevant (attended) versus task irrelevant (not attended). Both left and right hemisphere sources are evident in the field patterns when the grating was task relevant. Only a left hemisphere source is evident when the grating was task irrelevant.

2^{o} LOWER RIGHT QUADRANT

Empirical Fields **Theoretical Fields**

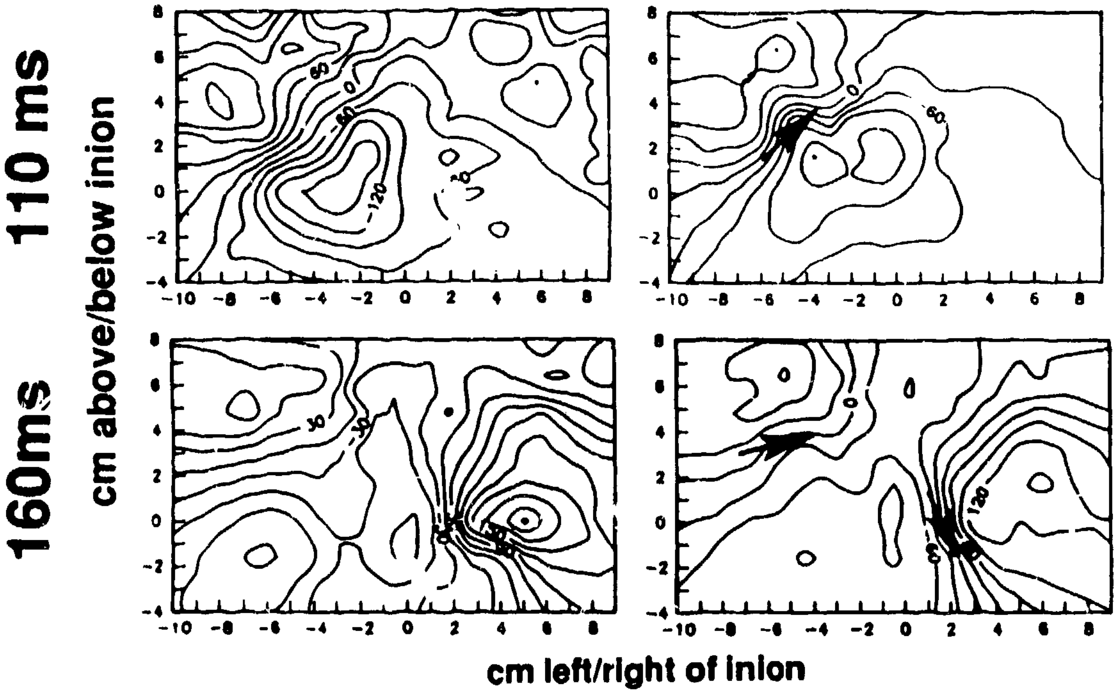

Contralateral Effects--110 ms

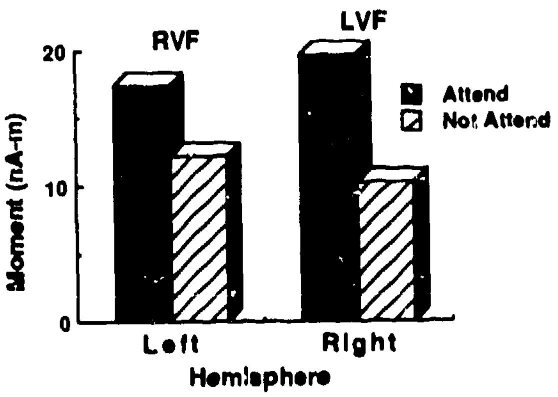

Ipsilateral Effects--160 ms

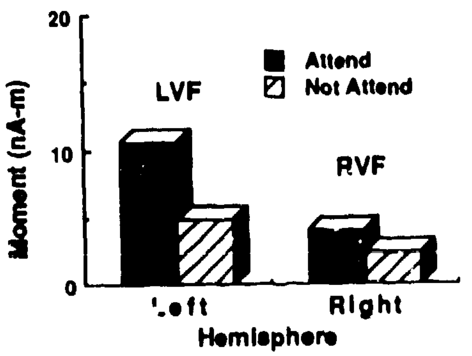

MONTE CARLO ERROR ANALYSES

LOWER RIGHT QUADRANT--160 ms

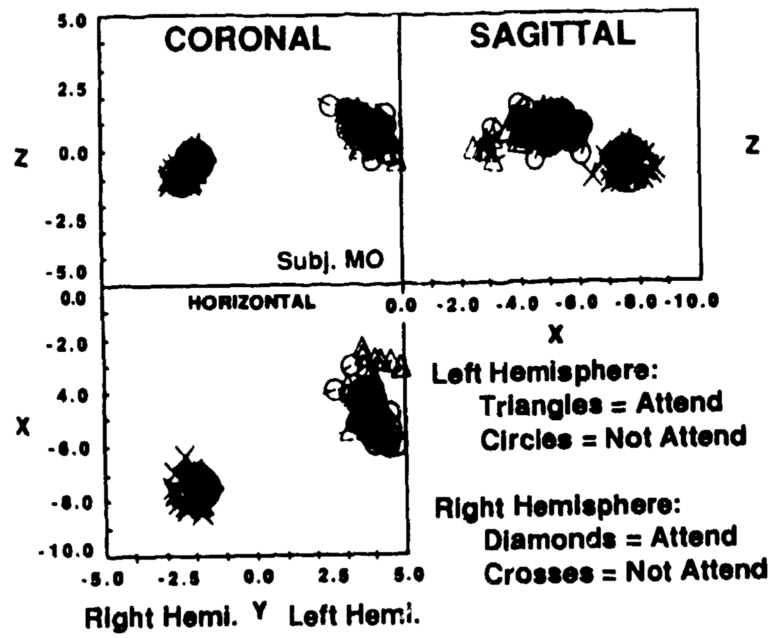

LOWER LEFT QUADRANT--160 ms

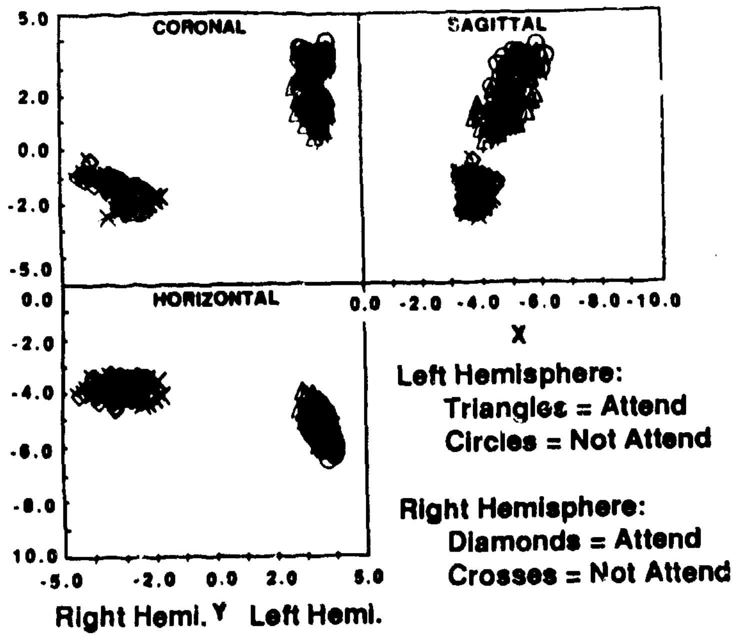

7° RVF HORIZONTAL MERIDIAN--150 ms